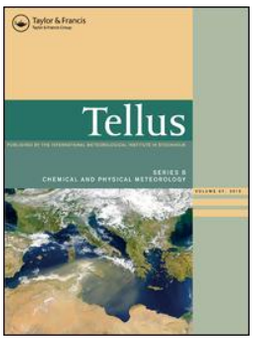

Tellus B: Chemical and Physical Meteorology

ISSN: (Print) 1600-0889 (Online) Journal homepage: https://www.tandfonline.com/loi/zelb20

The origin of Arctic precipitation under present and glacial conditions

S. J. Johnsen, W. Dansgaard & J.W.C. White

To cite this article: S. J. Johnsen, W. Dansgaard & J.W.C. White (1989) The origin of Arctic precipitation under present and glacial conditions, Tellus B: Chemical and Physical Meteorology, 41:4, 452-468, DOI: 10.3402/tellusb.v41i4.15100

To link to this article: https://doi.org/10.3402/tellusb.v41i4.15100

Tellus (1989), *41B*, 452–468

The origin of Arctic precipitation under present and glacial conditions

By S. J. JOHNSEN, *Science Institute, University of Iceland, Reykjavik, Iceland,* W. DANSGAARD, *Geophysical Institute, University of Copenhagen, Haraldsgade 6, DK-2200 Copenhagen, Denmark* and J. W. C. WHITE, *Laboratoire de Geochimie Isotopique, LODYC (UA CNRS 1206) CEA/IRDI/DESICP, Departement de Physico-Chimie, 91191 Gif sur Yvette, Cedex, France, and Geochemistry Department, Lamont-Doherty Geological Observatory, Columbia University, Palisades, New York 10964, USA*

(Manuscript received 9 November 1987; in final form 26 May 1988)

ABSTRACT

At low altitude locations, the deuterium excess $d = \delta D - 8\delta^{18}O$ in precipitation generally varies with the season in antiphase with the δ's. In the high-altitude regions of the Greenland ice sheet, however, d in the snow varies with only a few months time lag behind the δ's. A model for d values in Greenland precipitation is developed on the basis of Rayleigh condensation/sublimation with due account taken of kinetic effects during both evaporation of sea water and sublimation. The model predicts that the initial mixing ratio w_{so} in precipitating air determines the slope of the d versus δ relationship at late stages of the precipitation process, and that the sea surface temperature T_s in the source area of the moisture only influences the d level. The generally high d-values in ice sheet precipitation are compatible only with high values of w_{so} and T_s, which suggests the subtropical part of the North Atlantic Ocean as a dominating moisture source for ice sheet precipitation. This is supported experimentally: when the model is run with monthly w_{so} and T_s mean values oberved at Ship E (35°N, 48°W), it reproduces the high d level, the amplitude of the seasonal d variations, and the few months phase difference between d and δ on the ice sheet. None of these features can be reproduced with a local, high-latitude moisture source.

Detailed isotope analyses of ice core increments, spanning several abrupt climatic shifts under glacial conditions, show close to present d values during the cold phases, but lower d values during the mild phases. This feature is discussed in the light of the model experiments.

1. Introduction

This work treats the isotopic composition of precipitation at high northern latitudes, denoted by δ, which is the relative deviation in per mille (‰) of the deuterium or oxygen-18 concentration in a water sample from that in Standard Mean Ocean Water (SMOW). For annual precipitation at high latitude ocean islands and coastal locations, the relationship between δD and $\delta^{18}O$ is given by

$$\delta D = 8.0\delta^{18}O + 10‰, \quad (1)$$

the so-called Meteoric Water Line (Craig, 1961; Dansgaard, 1964).

There are several striking features of the observed distribution of $\delta^{18}O$ in the snow pack on the Greenland ice cap: firstly, the $\delta^{18}O$ versus surface elevation (z) gradient, $\partial\delta/\partial z$, is close to $-0.6‰/100$ m over most of Greenland (Epstein and Langway, 1959; Dansgaard, 1961); secondly, $\delta^{18}O$ varies regularly with latitude (λ), $\partial\delta/\partial\lambda$ being $-0.54‰$ per °lat., which is close to the latitudinal gradient for precipitation at low elevation stations along the West Greenland coast (Dansgaard, 1961); thirdly, $\delta^{18}O$ is closely related to the local mean annual surface temperature T in degrees celsius (Dansgaard et al., 1973):

$$\delta^{18}O = 0.62T - 15.25‰. \quad (2)$$

This relation holds for $T < -14°C$, i.e., for latitudes from 65°N to 77°N and at elevations between 1700 m and 3100 m. The area east of the main ice divide is only sparsely represented, though. A similar relationship exists in Antarctica for $T < -20°C$ (Lorius et al., 1969; Dansgaard et al., 1973; Lorius, 1983).

The features mentioned above suggest (i) that the distribution of temperature and mean δ values of precipitation on most of the Greenland ice cap are governed by the same environmental parameters; (ii) that the source area of the moisture, which successively fell as snow on the ice cap, is most probably the same for all ice cap

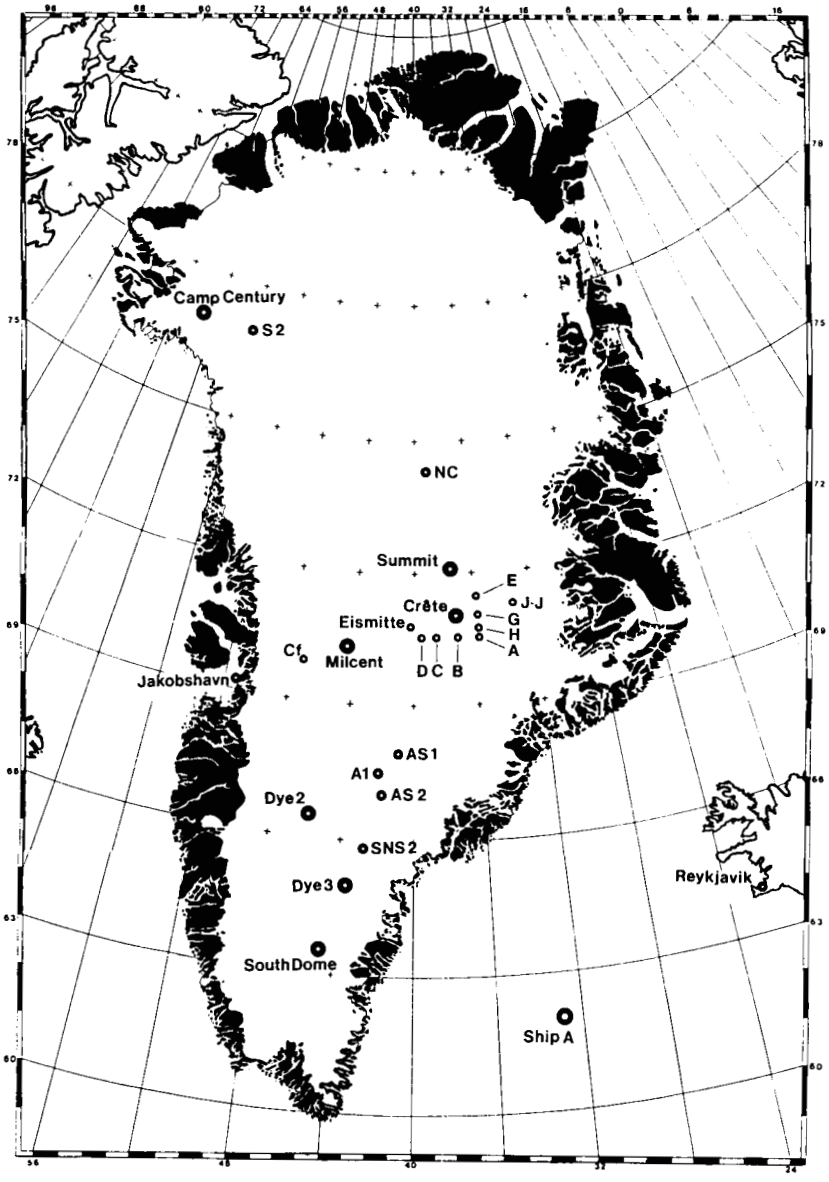

Fig. 1. Drill sites on the Greenland ice sheet.

stations, at least in South and West Greenland; (iii) that the same holds true for West Greenland coastal stations (an important local moisture source would reduce the latitudinal gradient); (iv) that the main part of the precipitation on the ice cap is formed close to the site of deposition.

In contrast, Fisher and Alt's (1985) model ascribes Arctic precipitation to moisture originating from, in principle, all latitudes north of the sub-tropical high pressure belt, but the model does not consider precipitation at high elevations.

A hint to solving the moisture source problem may be found by considering the deuterium excess

$$d = \delta D - 8\delta^{18}O, \quad (3)$$

which is close to 10‰ for precipitation in high-latitude coastal areas, cf. eq. (1). In non-equilibrium processes in the water cycle, kinetic effects cause changes in d, and need to be considered to explain both the usual d-value of 10‰ (Craig, 1961; Dansgaard, 1964; Merlivat and Jouzel, 1979) and the slope of 8.0 of the best linear fit to all data plotted in a δD versus $\delta^{18}O$ diagram (Jouzel and Merlivat, 1984). Jouzel et al. (1982) measured the deuterium excess along the ice core from Dome C, East Antarctica, and interpreted an increase in d from 4 to 8‰ across the Pleistocene to Holocene transition as a result of higher relative humidity above the ocean (i.e., smaller kinetic effect in the evaporation process) under glacial conditions than in the post-glacial epoch.

In 1979–81, a 2037 m ice core was drilled to bedrock at Dye 3, Southeast Greenland (Fig. 1), under the American–Danish–Swiss joint effort GISP (Greenland Ice Sheet Program; Langway et al., 1985). An abrupt drop in $\delta^{18}O$ at 1786 m depth, dated at 10,720 ± 150 years B.P. (Hammer et al., 1986), marks the transition to ice deposited during the Wisconsin/Würm glaciation. This ice is generally 6 to 7‰ lower in $\delta^{18}O$ than Holocene ice, but it is further characterized by many more or less abrupt shifts in δ (Fig. 2), which have been reconciled with similar features in the δ record along the deep ice core from Camp Century, Northwest Greenland (Dansgaard et al., 1982). This suggests that the climatic conditions in the North Atlantic Ocean oscillated between two quasi-stationary stages (Dansgaard et al., 1971, 1984). Similar abrupt shifts have been found in the Grande Pile pollen profile from northeastern

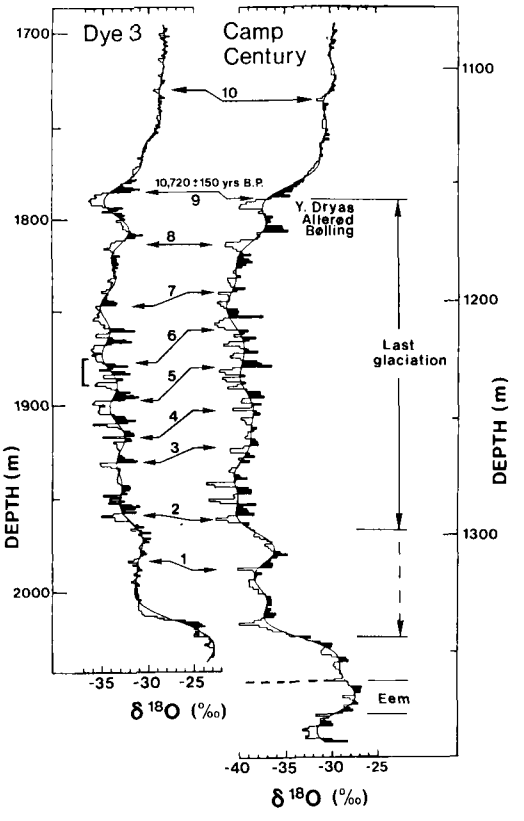

Fig. 2. $\delta^{18}O$ profiles along the deepest, ~300 m, of the two surface to bedrock ice cores from the Greenland ice sheet. The last glaciation is revealed by δ's below −31‰ in the Dye 3 core, and below −35‰ in the Camp Century core. The arrows point at common features suggesting layers of simultaneous deposition. The three δ-oscillations marked on the left-hand side of the Dye 3 record have been the object of detailed studies, see Fig. 8.

France (Woillard and Mook, 1981) and in the abundance of planktonic foraminifera in Greenland waters (Ruddiman and McIntyre, 1981). They were probably associated with considerable advances and retreats of the polar front, and thereby of the sea ice cover, similar to those during the last glacial climatic oscillation, Bølling/Allerød-Younger Dryas (Ruddiman and McIntyre, 1981).

Three of the numerous oscillations (in the depth interval 1975–1889 m) have been analyzed in great detail for chemical composition (Finkel and Langway, 1985), ^{10}Be (Beer et al., 1984),

CO_2 (Stauffer et al., 1984), $\delta^{18}O$ and dust content (Dansgaard et al., 1984; Hammer et al., 1985). All of these parameters change almost simultaneously, indicating drastic shifts in the entire environment.

2. Data

2.1. Recent deposits

In addition to the Dye 3 deep core, numerous ice cores to depths between 10 and 400 m were drilled or handaugered in the period 1971–85 under GISP (Fig. 1). They offer an opportunity to re-establish the mean $\delta^{18}O$ versus mean surface temperature T (represented by the temperature at 10 or 20 m depth) using the comprehensive GISP material, collected and handled by one and the same technique.

These data are plotted in Fig. 3. The best linear fit to stations in South and West Greenland, is

$$\delta^{18}O = (0.67 \pm 0.02)\,T - (13.7 \pm 0.5)‰,$$

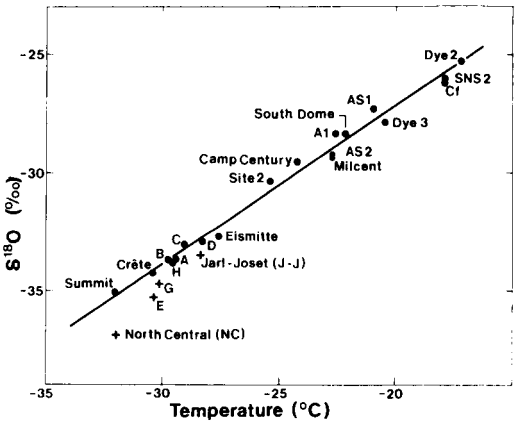

Fig. 3. Mean $\delta^{18}O$ of snow deposited on the Greenland ice sheet plotted against the annual mean surface temperature as represented by the temperature at 10 or 20 m depths.

i.e., not far from the previously established relationship (2). A significant part of the precipitation at ice cap stations in the low accumulation

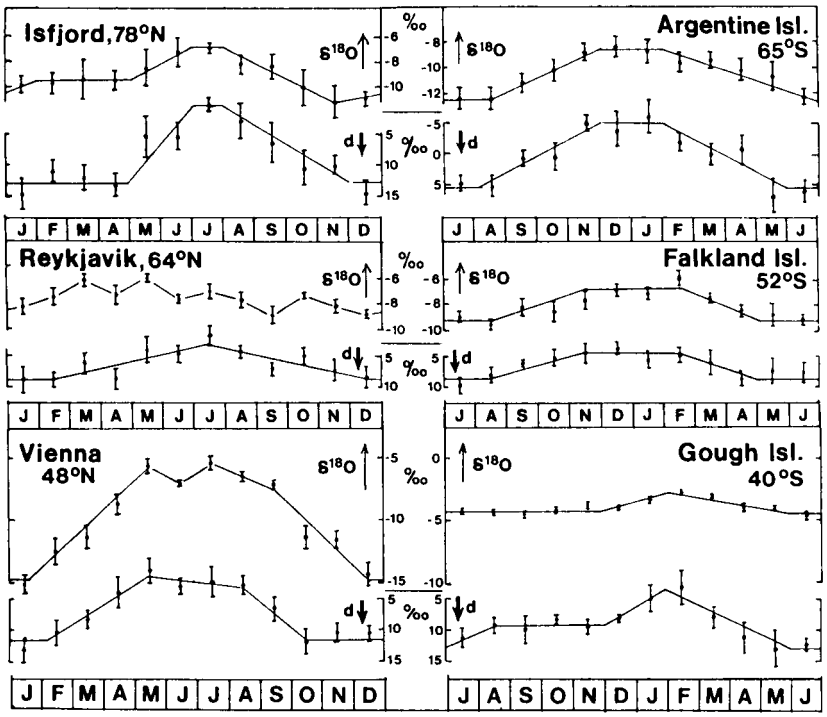

Fig. 4. Monthly mean $\delta^{18}O$ and deuterium excess (d) values of precipitation at six low-altitude stations. The two parameters generally vary in antiphase (notice the reversed d-scale) with extremes in summer and winter. Data from the IAEA/WMO precipitation survey.

area in Northeast Greenland originates from the west (Clausen et al., 1987) and is therefore excessively depleted in heavy isotopes. These locations are shown by the crosses in Fig. 3.

It has been known for many years that the isotopic composition of precipitation varies in a seasonal cycle with maximum δ's in summer, minimum δ's in winter (Epstein and Langway, 1959). This cycle is particularly pronounced at locations far from the source area of the moisture, and has been used to determine the annual stratigraphy of snow and ice in the ice sheets, and thereby for absolute dating of ice cores (e.g., Hammer et al., 1978; Clausen et al., 1987). In one case, these cycles have been counted through most of the Holocene (Hammer et al., 1986), for accurately dating of the Pleistocene to Holocene transition (shown by arrow 9 in Fig. 2).

Less attention has been paid to the fact that the deuterium excess, as given by eq. (3), varies in antiphase with the δ's at a given low altitude station (Yurtsever and Gat, 1981), see Fig. 4.

Consequently, the mean isotopic composition of monthly precipitation follows a line with slope less than 8 in a δD versus $\delta^{18}O$ diagram, although most of the annual mean values are close to the line described by eq. (2).

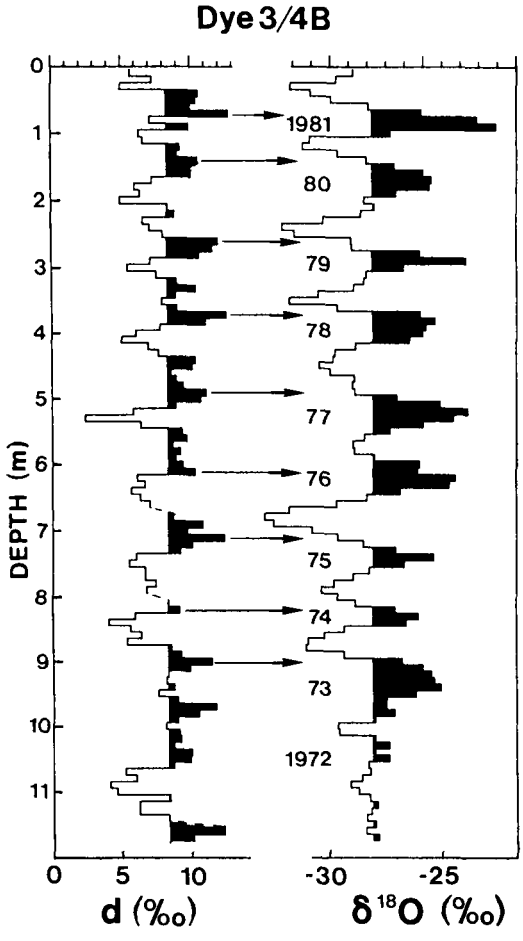

Fig. 5. Right: seasonal $\delta^{18}O$ cycles at station Dye 3/4B, southeast Greenland (elevation 2491 m) through nearly 12 years. A maximum occurs generally around 1st of August, minimum around the 1st of February. Left: the deuterium excess also varies with the season, but in contrast to low-altitude stations *not* in antiphase with δ. Maximum deuterium excess occurs usually in autumn.

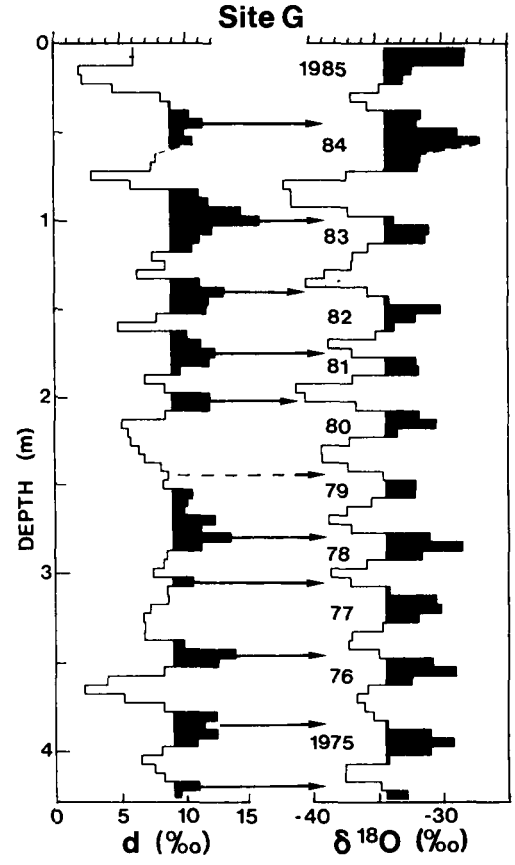

Fig. 6. Seasonal $\delta^{18}O$ and deuterium excess cycles at Site G (elevation 3098 m), some 700 km NNE of Site 4B.

However, the isotopic composition of the snow and ice on the Greenland ice cap shows different features.

Two continuous series of firn samples were collected, one in 1983 at site 4B (65°10′N, 43°56′W) in the Dye 3 area, Southeast Greenland, and another one in 1985 at site G (71°09′N, 35°50′W), in Central Greenland, cf. Fig. 1. Isotope analyses were done with analytical uncertainties of $\pm 0.3‰$ for δD, and $\pm 0.06‰$ for $\delta^{18}O$. The estimated accuracy of d is $\pm 0.8‰$. The data showed, firstly, that both of the series span 10–11 years of snow deposition (cf. the right-hand sides of Figs. 5, 6) and, secondly, that d (left-hand sides) varies in a seasonal cycle, but *not* in antiphase with $\delta^{18}O$. The deuterium excess is generally highest in autumn and lowest in spring, and the amplitude is approximately 4‰. The two records have these featues in common, which is important, because it suggests that any given and widespread snowfall on the ice sheet gives snow of essentially the same deuterium excess at the two sites, in spite of their more than 6‰ difference in $\delta^{18}O$.

Due to the approximately 90° phase difference between δ and d, the individual samples cannot be expected to follow a line with slope less than 8 when plotted in a δD versus $\delta^{18}O$ diagram, but, in the ideal case, rather an ellipse with a main axis parallel to the Meteoric Water Line. The upper part of Fig. 7 shows a plot based on 230 samples from site 4B. The two last lines of Table 1 give characteristics of the best linear fits to the data points of the two series of firn samples.

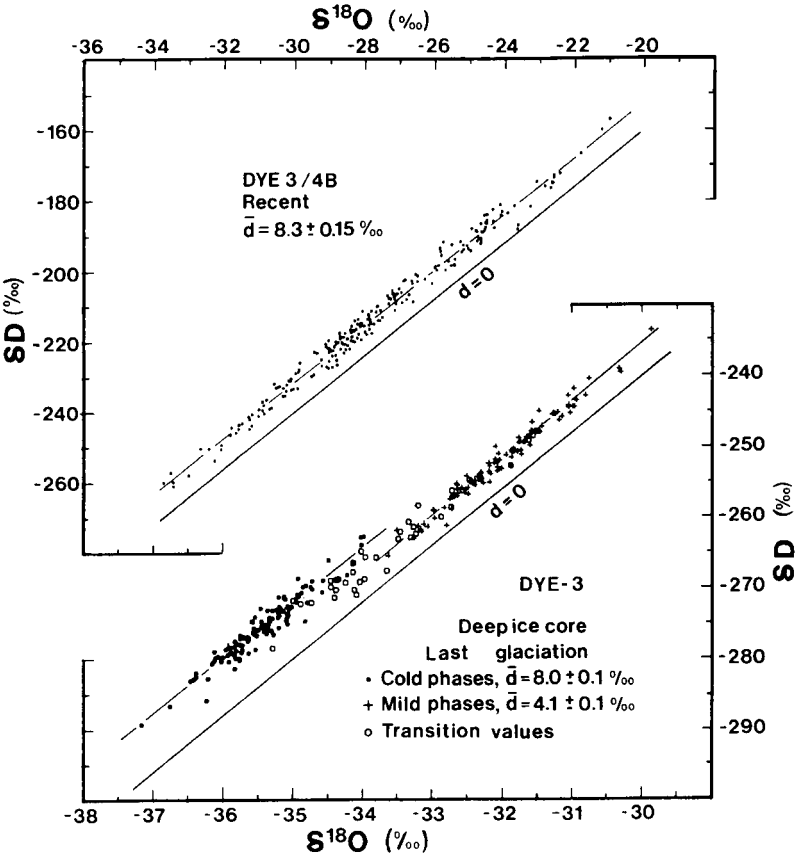

Fig. 7. Top panel: the isotopic composition of 230 firn samples from Dye 3/4B plotted in a δD versus $\delta^{18}O$ diagram (scales on top and to the left). The broken line is the best linear fit. The full line is $\delta D = 8\delta^{18}O$, i.e., $d = 0$. Bottom panel: similar plot of the data shown in Fig. 8 (notice the *extended* scales at the bottom and to the right).

None of the slopes deviate significantly from 8.0, and the mean deuterium excess d is essentially the same.

2.2. Pleistocene deposits

Unfortunately, ice from the glaciation contains no information on seasonal δ cycles at that time. They have all been obliterated by molecular diffusion (Johnsen, 1977). No matter how thin a sample one cuts from the Dye 3 ice core less than 250 m from bedrock, its isotopic composition will represent a mean value of several years of snow deposition.

Nevertheless, the three oscillations in the depth interval 1875–1889 m marked to the left of the Dye 3 δ profile in Fig. 2 have been sampled in great detail for isotope analyses. The results are shown in the top and middle sections of Fig. 8, in which the youngest sample is plotted to the left, the oldest one to the right ("time goes towards the left"). The mild phases ($\delta^{18}O > -33.5‰$) and the cold phases ($\delta^{18}O < 33.5‰$) are shaded light and dark, respectively, and separated by periods of transition with either a clear trend in δ, or with δ's that shift between the two groups.

In view of the smoothing effect of diffusion, the cold to mild phase transitions seem to have been very abrupt, lasting perhaps only a decade or so. On the other hand, the transitions from mild to cold phases went on more gradually.

As shown in the lower section of Fig. 9, the deuterium excess changed essentially in antiphase with the δ's (notice the reversed d-scale), although it seems, as if the shift in deuterium excess occurred prior to the δ-shift in the cold to mild phase transitions (e.g., the shift at 1884 m depth), and after the δ-shifts in the mild to cold phase transitions. This feature is also characteristic of the insoluble dust concentration in the ice (Hammer et al., 1985; Dansgaard et al., 1984).

A less detailed sampling would have given a false impression of a δD to $\delta^{18}O$ relationship with a slope less than 8. However, when the δ's of all the 120 cold phase samples, and those of all the 99 mild phase samples are plotted individually in a δD versus $\delta^{18}O$ diagram (lower part of Fig. 7), two different lines appear, both of them with slopes that do not deviate significantly from 8.0. The mean values $\bar{d}$ of the deuterium excess for the cold and mild phases are significantly different, see Table 1.

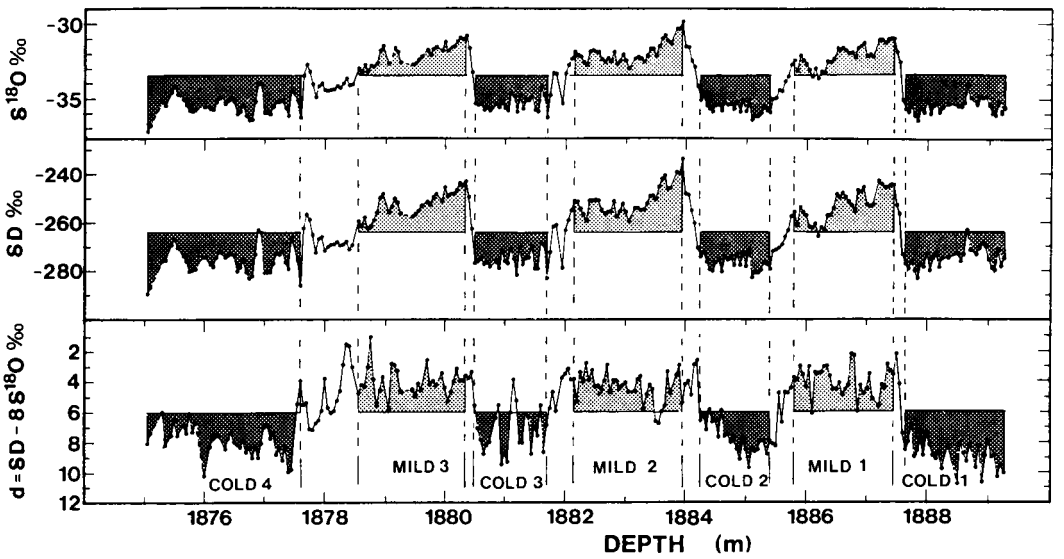

Fig. 8. Detailed profiles of $\delta^{18}O$ (top), δD (middle), and deuterium excess (bottom, notice the reversed scale) through the depth interval 1875–1889 m in the Dye 3 deep core. The light-shaded increments are the three peaks marked in Fig. 2. The cold-to-mild phase transitions are more abrupt than the reverse transitions.

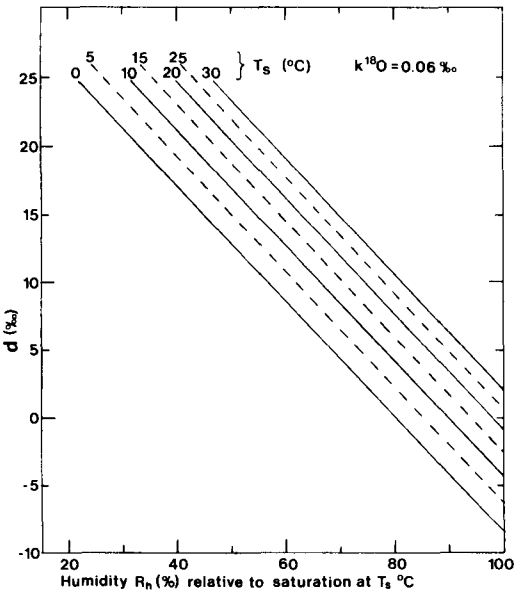

Fig. 9. Deuterium excess d_{vo} in moisture evaporated from an ocean surface of temperature T_s into air of humidity R_h relative to saturation at T_s.

Surprisingly enough, the deuterium excess was much closer to present ice sheet values (8.3‰ at Dye 3; 8.8‰ at Site G) in the cold phases (8.0‰) than in the mild phases (4.1‰).

3. Modelling

The model described below was designed in order to explain the deuterium excess data now available from Greenland ice cores. We first consider the isotopic fractionation processes during the evaporation from the ocean surface, then the transport of an air parcel from the source area of its moisture to the ice sheet, and finally the isotopic fractionation in the condensation/sublimation processes during the entire transport.

3.1. Evaporation

The ocean is assumed to have the composition of SMOW. In that case, the isotopic composition δ_{vo} of the initial vapour is calculated according to Merlivat and Jouzel (1979):

$$\delta_{vo} = \frac{1}{\alpha_e}\frac{1-k}{1-kR_h} - 1, \tag{4}$$

α_e being the isotopic equilibrium fractionation coefficient of either D or ^{18}O at the ocean surface temperature T_s; k is a variable parameter describing the kinetic fractionation effects at the air–ocean boundary, and R_h (unconventionally) the humidity of the air relative to air saturated at T_s.

Using the Brutsert evaporation model, Merlivat and Jouzel (1979) derived $k^{18}O$ values of 6–7‰ for a smooth evaporation regime, and 3–4‰ for a rough regime. They also showed that $kD/k^{18}O = 0.88$, and they defined a rough regime for wind speeds higher than 7 m/s 10 m above the ocean surface. According to Eriksson and Bolin (1964), 95% of present day ocean surface has a smooth regime. In this work, we therefore use $k^{18}O = 6‰$.

The deuterium excess d_{vo} of vapour evaporating over a wide range of environmental conditions can be determined by calculating $\delta_{vo}D$ and $\delta_{vo}{}^{18}O$ separately. The results are plotted in Fig. 9, showing that d_{vo} decreases (i) when the humidity over the ocean increases, or (ii) when the temperature of the surface ocean decreases. Furthermore, d_{vo} decreases for increasing wind speeds over the ocean, because lower d_{vo} is obtained when using lower values of k. Note also that with humidities of 70 to 80%, and temperatures of 20 to 25°C, i.e., average values for the subtropical oceanic evaporation belts, d_{vo} is about +10‰, which is the present average d-value of continental precipitation defining the Meteoric Water Line.

Table 1. *Characteristics of best linear fits to the isotopic composition of ice sheet sample series plotted in a δD versus $\delta^{18}O$ diagram*

Site of collection	Climatic phase	No. of samples	Slope	Mean d (‰)
Dye 3, core	glaciation, cold	120	7.8 ± 0.2	8.0 ± 0.1
Dye 3, core	glaciation, mild	99	8.1 ± 0.1	4.1 ± 0.1
Dye 3/4B	present, warm	230	7.94 ± 0.06	8.3 ± 0.15
Site G	present, warm	84	8.0 ± 0.1	8.8 ± 0.3

3.2. *Vapour transport*

A parcel of humid air is now cooled off to the dew point T_d (Fig. 10). Further cooling results in condensation, and the condensate is removed immediately (Rayleigh condensation).

At temperature T_o, the air parcel is assumed to enter a cyclonic system, and it starts to ascend. The transport to the coast of Greenland and further to ice cap stations at high elevation H_s is assumed to take place as follows. The air parcel is lifted in steps of Δh from the surface to a specified height under moist adiabatic cooling, supplied by radiative cooling, until it reaches the coast of Greenland. The contact with the coastal region may happen in South Greenland or in North Greenland (SGrl. and NGrl. in Fig. 10). From there on, the air parcel is lifted under moist adiabatic cooling to the site of snow collection (elevation H_s), where the precipitating clouds are h_p above the surface. h_p is assumed to be 500 m in Central Greenland (elevation 3200 m), and to vary according to

$$h_p = 500 + \varphi(3200 - H_s), \tag{5}$$

φ being a factor to be determined by tuning the model to reproduce the observed δ variation with surface elevation (-0.62‰ per 100 m). The air parcel is assumed to cool off adiabatically and by outgoing radiation to such an extent that the lifting over the ice cap gives a calculated $\delta^{18}O$ value of the precipitation equal to the observed one. Thereby, the temperature of formation of the collected snow becomes an output of the model, and the problem of specifying it as an input is avoided.

The radiative cooling is quantified by extracting an energy of ΔQ Joule per kg air in each step:

$$\Delta Q = q \cdot \Delta h, \tag{6}$$

q being a constant to be determined by trial and error.

Other modes of transport were considered, but did not produce significantly different results.

3.3. *Condensation/sublimation*

The equations describing the isotopic fractionation in a Rayleigh condensation/sublimation process are

$$\left.\begin{aligned} \frac{d\delta_v}{\delta_v + 1} &= (\alpha - 1)\frac{dw_s}{w_s} + \frac{d\alpha}{\alpha} \\ \delta_c &= \alpha\,(\delta_v + 1) - 1 \end{aligned}\right\}, \tag{7}$$

δ_v and δ_c being the delta values (δD or $\delta^{18}O$) of the vapour and the condensate/sublimate, respectively, α the fractionation factor for either isotope at the temperature T of the air parcel, and w_s the mixing ratio (g H_2O/kg air). Eq. (7) are solved numerically for each heavy isotopic component, thus describing the isotopic composition of the precipitation as the cooling proceeds.

The first part of the Rayleigh process, i.e., till the air has reached a temperature $T_f = -5$°C, is assumed to take place under vapour–liquid equilibrium conditions, and α is put equal to α_e, i.e.,

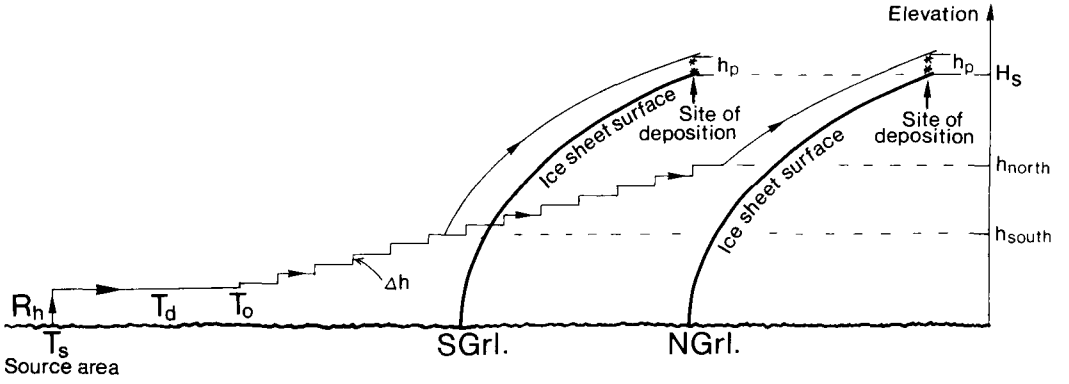

Fig. 10. The moisure transfer from the source area to the Greenland ice sheet considered in the model is based on Rayleigh condensation and takes kinetic effects into account, during both evaporation and sublimation. T_s is the temperature of evaporating sea water, see text for further details.

the equilibrium fractionation factors for HDO and $H_2{}^{18}O$ measured by Merlivat and Nief (1967) and Majoube (1971), respectively.

As soon as the cooling has reached a point from which the solid phase plays an important role, the situation gets considerably more complicated.

Jouzel and Merlivat (1984) have shown that Rayleigh sublimation (their RM model) with snow formation under equilibrium conditions leads to a strongly variable and much too high deuterium excess d in the precipitate at later stages of the process. By introducing kinetic effects in the vapour-to-snow sublimation process, they manage to eliminate this deviation (their RMK model). By adjusting the level of supersaturation δ_i as a function of temperature, the RMK model also explains the linear relationship, observed in East-Antarctica, between δD and temperature T_i on top of the inversion layer at the site of deposition. T_i is then assumed to be the actual temperature during the snow formation.

In order to describe the kinetic effect in the sublimation process, Jouzel and Merlivat (1984) introduce the kinetic fractionation coefficient α_k. The effective fractionation factor

$$\alpha = \alpha_k \cdot \alpha_e \tag{8}$$

is then used in eq. (7) instead of the equilibrium fractionation factor α_e. Neglecting the form factor for the snow crystals, they write

$$\alpha_k = \frac{S_i}{1 + \alpha_e (S_i - 1)\, D/D'}, \tag{9}$$

D and D' being the diffusion constants in air for the light and the heavy isotopic components, respectively. Their ratio D/D' is 1.0285 for $H_2{}^{18}O$ and 1.0251 for HDO. α_k is always less than unity. S_i is in fact the supersaturation ratio at the temperature of the snow crystals, which may have a higher temperature than the ambient air due to the latent heat released during sublimation.

In accordance with Jouzel and Merlivat (1984), we write S_i as a simple function of the sublimation temperature T°C:

$$S_i = c - FT, \tag{10}$$

c and F being constants to be determined by trial and error. Furthermore, by assuming vapour–liquid equilibrium down to only $T_f = -5$°C, we allow for the precipitation of super-cooled droplets sticking to the falling snow that forms higher in the cloud system.

3.4. *Tuning*

The model has been tested for various combinations of the parameters c, F and T_f, and for various parameters R_h and T_s in the source region. We have studied the model prediction of the deuterium excess d during the entire condensation/sublimation process. Independent of the mode of lifting, it turns out that if we assume the range of d (4 to 12‰) observed at stations 4B and G as being typical for the entire ice sheet, narrow limits are put on possible values of the model parameters c, F, T_f, R_h and T_s. Thus, c may vary between 1.00 and 1.04; F from 0.005 to 0.007°C^{-1}; T_f from 0°C to −10°C; R_h from 70 to 90%; and T_s from 18 to 27°C. The values for c and F were chosen to be 1.025 and 0.006, respectively.

The constraint on T_s excludes high-latitude moisture source regions as major contributors to the precipitation at high elevations on the Greenland ice cap. Even optimum tuning of the model with the Weathership A area (62°N, 33°W), not far from South Greenland (Fig. 1), as a moisture source leads to deuterium excess values at Site G far from those observed. For the moment, we tune the model using the subtropical Weathership E (35°N, 48°W) area as a source of moisture.

As to the φ factor in eq. (5), a value of zero corresponds to constant height (500 m) of snow formation over the entire ice cap surface, and a value of unity corresponds to no lifting at all, and hence no adiabatic cooling. The φ factor was chosen at 0.2, which completely accounts for the observed isotopic altitude effect, $\partial\delta^{18}O/\partial z = -0.62$‰ per 100 m, regardless of the adiabatic to radiative cooling ratio during the passage from the coast to the site of deposition.

Finally, the q factor in eq. (6) was chosen (at 19 J/kg·m) so that the model reproduces the observed $\delta^{18}O$ values both at Milcent and at the coastal Jakobshavn (cf. Fig. 1) on the Mid-Greenland coast (−29.3‰ and −16‰, respectively), when run with Ship E as a moisture source. The latitudinal $\delta^{18}O$ gradient along the coast, calculated with this q value, is −0.5‰ per °lat., in good agreement with the observed

$-0.45‰$ per °lat. (Dansgaard, 1961), and with that on the ice sheet ($-0.54‰$ per °lat.). The same procedure with high latitude moisture sources leads to much too high latitudinal gradients, e.g., $-0.9‰$ per °lat. when starting out from Weathership A.

As mentioned in Subsection 3.2 the temperature of formation of the collected snow, T_p, comes out as an output of the model. Taking the Ship E area as a source, a linear relation is found between the annual mean δ value $\bar{\delta}$ and the annual mean of T_p:

$$T_p = 1.04\,\bar{\delta}^{18}O + 10.6°C.$$

At high altitude stations, the corresponding ground temperature during snow storms, T_g (not to be mistaken for T in eq. (2)), is 4 to 5°C higher.

At Eismitte (Fig. 1), the model predicts T_g for the coldest month 15°C warmer than the mean surface temperature in that month. This is in accordance with the observation made by the Alfred Wegener expedition to Central Greenland 1930–31, that the mean surface temperature in winter is influenced by a strong inversion, whereas the warm air masses that bring the winter snow cause temporary temperature increases of up to 20°C (Loewe, 1936).

4. Results and discussion

4.1. Isotopic composition of initial vapour and first stage precipitation

In order to determine the initial deuterium excess d_{vo} of the vapour from the Ship A and Ship E areas, the model was run with monthly values of the parameters R_h and T_s (World Survey of Climatology, 1984; IAEA/WMO, 1963–76) from the two ships, and calculated by eq. (4), as shown by the bold face curves in the top and bottom sections of Fig. 11, respectively. In both cases, d_{vo} has a minimum in June, but vapour from the high-latitude areas (Ship A) has a distinct d_{vo} maximum in Janaury, whereas d_{vo} in subtropical vapour essentially keeps constant around 12‰ from August through February.

The dashed curves in Fig. 11 show the deuterium excess d_{po} in the first precipitation given off from the parent vapour, as calculated by eq. (7). In both cases, d_{po} varies essentially in phase with d_{vo}.

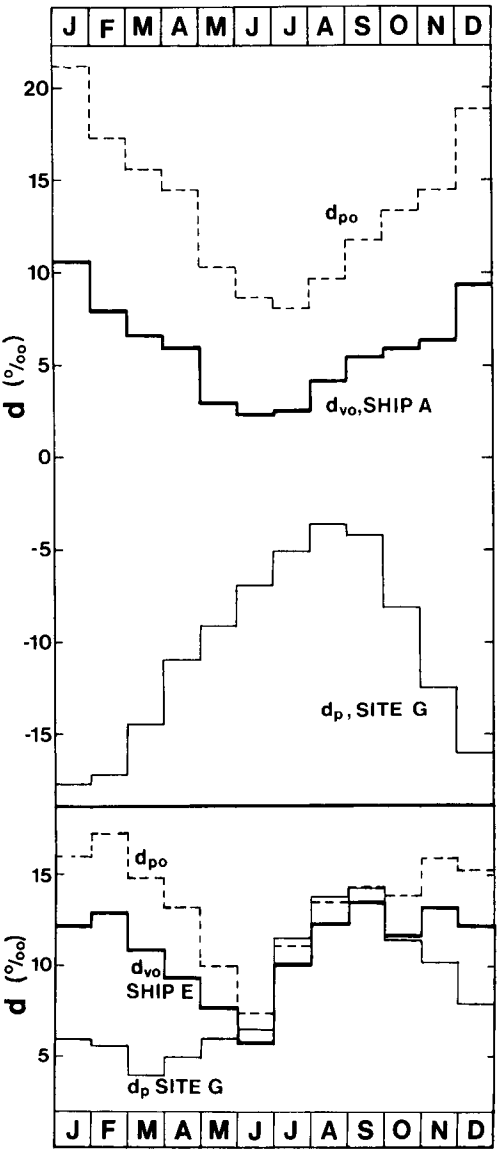

Fig. 11. Top section: seasonal variation of initial deuterium excess d_{vo} in vapour from the high-latitude Ship A area (heavy curve); deuterium excess d_{po} in first stage precipitation from such vapour (dashed curve); deuterium excess d_p in precipitation at the high elevation station G on the Greenland ice sheet (full, thin curve) after condensation/sublimation through the vapour transport mechanism outlined in Fig. 10. Bottom section: same as above, but starting out with vapour from the subtropical Ship E area.

4.2. Precipitation at later stages

Two important properties of the model have emerged, cf. Fig. 12, which shows the d_p versus $\delta^{18}O$ relationship calculated with the w_{so} and T_s values listed to the right.

(a) For any given set of parameters, c, F and T_f within the limits given in Subsection 3.4, the initial mixing ratio w_{so} controls the general slope of the d_p versus $\delta^{18}O$ curve, and thereby the slope of the δD versus $\delta^{18}O$ curve. Lower w_{so} results in higher slopes, essentially independent of the ocean temperature T_s in the source area.

(b) Changing T_s for a given w_{so} (or dew point) causes a parallel shift of the d versus $\delta^{18}O$ curve. Note, however, that w_{so}, T_s and R_h (the humidity relative to T_s) are not mutually independent variables. Holding w_{so} constant and lowering T_s, for example, necessarily raises R_h. As shown in Fig. 9, lower T_s and higher R_h act in concert and, in this example, result in sharply lowered d values. Thus, the model result that w_{so} controls the slope of the δD versus $\delta^{18}O$ curve has added significance. If isotopes in precipitation define a single line, implying a constant w_{so}, any change in d caused by a change in T_s will be magnified by the concurrent change in R_h. This explains why, in Fig. 12, a 2°C change in T_s results in a 4‰ change in d, whereas in Fig. 9 a 2°C change in T_s with humidity held constant (requiring a change in w_{so}) results in only a 1 to 2‰ change in d.

Optimum tuning of the model, i.e., the tuning that results in the best reproduction of the observed d_p-values, leads to the exemplified dashed and full curves in Fig. 13, showing the d_p versus $\delta^{18}O$ relationship calculated with the w_{so} and T_s values at Ship A and Ship E, respectively, as listed on the right. The dots refer to the individual Site G samples. The three rectangles (open, and with light and heavy shadow) envelope most of the observations at Dye 3/4B, Isfjord (Svalbard) and Reykjavik, respectively.

Obviously, the model has to start out with vapour mainly from a low-latitude source, in order to reproduce the high deuterium excess observed on the ice cap. In contrast, both low and high latitude sources may contribute to the precipitation at the low elevation stations, Reykjavik and Isfjord.

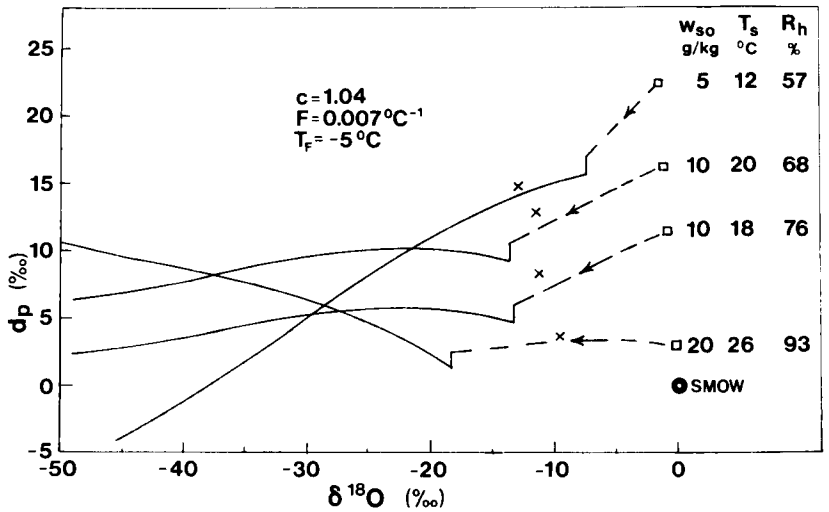

Fig. 12. Calculated deuterium excess d_p versus $\delta^{18}O$ in precipitation released by progressive Rayleigh-condensation/sublimation from air, which left the moisture source with the moisture content w_{so} (isotopic composition denoted by crosses), evaporated from an ocean surface of temperature T_s and isotopic composition SMOW. The composition of first-stage precipitation is denoted by squares. The dashed curves refer to condensation under water-vapour equilibrium during cooling to −5°C, the full curves to sublimation by further cooling under non-equilibrium conditions.

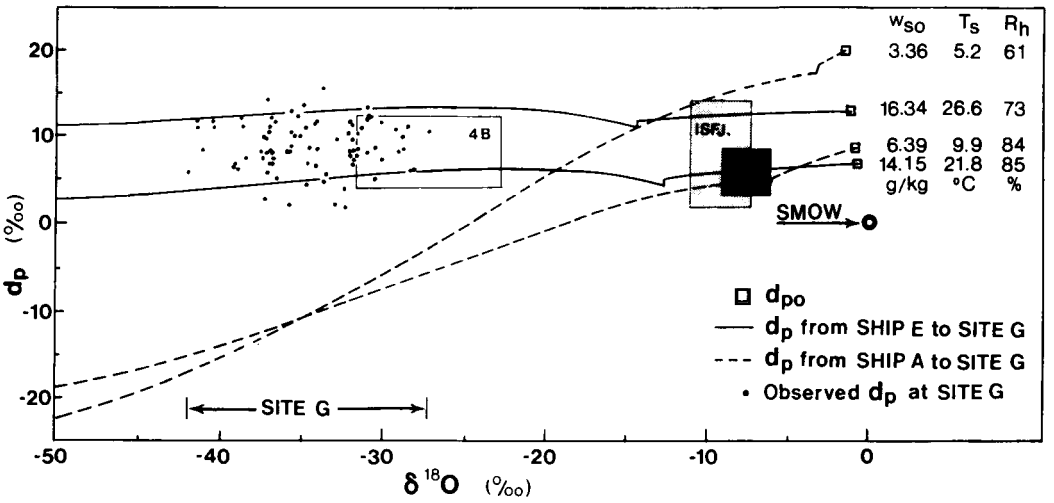

Fig. 13. As Fig. 12. The full and dashed curves are calculated with monthly mean values of w_{so} and T_s at Ship E and Ship A, respectively. The dots refer to measured composition of the individual samples from Site G (cf. Fig. 6). The open rectangle marks the typical d and $\delta^{18}O$ ranges observed in the snow pack at Site 4B (cf. Fig. 5), and the shaded rectangles those in precipitation at the low-elevation stations Isfjord and Reykjavik (cf. Fig. 4).

4.3. Seasonal d_p variations

Further evidence of ice cap precipitation originating mainly from low-latitude moisture, appears when we consider the seasonality in δ_p and d_p: Minimum δ_p in high latitude precipitation usually occurs around the 1st of February, and maximum around the 1st of August. Assuming a uniform distribution of precipitation throughout the year, the mean δ_p at an ice cap station in month no. i may therefore be approximated by

$$\delta_{pi} = \bar{\delta}_p - \Delta\delta_p \cos(2\pi(i - 1.5)/12),$$

$\bar{\delta}_p$ being the mean annual $\delta^{18}O$ value at the site of collection (−28.0‰ at Site 4B, and −34.5‰ at Site G), and $\Delta\delta_p$ the amplitude of the annual $\delta^{18}O$ cycle in falling snow, which is approximately 7‰ (Dansgaard et al., 1973).

The mean deuterium excess d_p in monthly precipitation of isotopic composition δ_{pi} is calculated using eqs. (3) through (10), and shown for Site G by the full thin curves in Fig. 11.

As the cooling proceeds, until the observed $\delta^{18}O$ values at Site G are reached, the model causes an inversion of the seasonality of d_{vo} in the high latitude case (Ship A) such that at Site G, the model predicts maximum d_p in August, and minimum d_p in January. The predicted drop in d_p during the cooling is approximately 13‰ in summer, and as much as 40‰ in winter. Thus, model calculations based on a high-latitude source region does not reproduce the observed seasonality at Site G and, in addition, it yields far too low deuterium excesses on the ice sheet. This is true regardless of the choice of parameters used in the model.

In contrast, starting out with vapour from a mid-latitude source region, such as the Ship E area, the model predicts d_p values at Site G, which range from 4.0‰ in March and 14.2‰ in September, depicting a distinct maximum in autumn, and an annual mean of 8‰. For Site 4B, the range is from 5.5‰ in March to 14.0‰ in September, with a mean d_p-value of 9.0‰.

The latter results based on a mid-latitude source region for the moisture are in good agreement with the observations at both Site G and Site 4B, regarding the annual mean, as well as the seasonal amplitude and the phase (see Figs. 5, 6).

The mean deuterium excess (+8‰) observed at the continental, high elevation sites G and 4B, is only compatible with initial air moisture content and sea surface temperature of ~11 g/kg and 20°C, respectively, which under present climatic conditions correspond to a vapour source region just north of the Atlantic subtropical anticyclones.

The realistic modelling of the latitudinal $\delta^{18}O$ gradient along the West Greenland coast (Subsection 3.3) suggests that mid-latitude moisture is also an important contributor to the precipitation at West Greenland coastal stations. However, in general, the available deuterium excess data from these stations do not allow a distinction between high and low latitude areas as moisture sources. One would expect that local waters contribute considerably. The d_{po} curve in the upper part of Fig. 11, valid for the first stage precipitation from moisture of high-latitude origin, defines high enough starting points to encompass the d_p variability observed at any of the stations covered by Fig. 4; furthermore, it varies in phase with d_p in Fig. 4. However, rigorous modelling of deuterium excess for coastal precipitation is difficult. Vapour may originate from a wide variety of latitudes, as suggested by Fisher and Alt (1985), and, in addition, sub-cloud isotopic fractionation processes associated with liquid precipitation further complicates the situation.

Nevertheless, the remarkable difference between mean d_p at Isfjord and Argentine Islands (8‰ and 0‰, respectively, cf. Fig. 4) suggests that the latter receives a considerable part of its precipitation from moisture evaporated under the cold (low T_s, cf. Fig. 9) and very rough regime ($k^{18}O = 3‰$ in eq. (4)) in the nearby Drake Strait, cf. Subsection 3.1.

4.4. *Moisture transport in cyclonic systems*

In contrast to East Antarctica (Lorius et al., 1985), most of the precipitation falling in Greenland is caused by cyclonic storms (Loewe, 1936). Usually, such cyclones originate in the North Atlantic Ocean south and east of Newfoundland. Prevailing winds in that area are from the south and west. They carry vapour that may have originated as far south as 35–40°N, i.e., still well north of the northern hemisphere Hadley cell. This vapour has therefore evaporated from a warm ocean, 18–26°C, and in areas of high mixing ratios w_{so}. In winter, however, cold dry winds from the North American continent reduce the relative humidity of the air and to some extent also the sea surface temperatures.

The cyclones form along the polar front. The major ones are normally fed by the so-called warm conveyor belt, which brings moist air originating as far south as 30°N directly into the cyclonic system (Green et al., 1966). As the cyclones move northward, they sweep the low-altitude humid air to higher altitudes, and precipitation forms. Eventually, the cyclones become occluded, and the warm conveyor belts disintegrate. From then on, little or no more water vapour enters the cyclonic system; the warm air is now trapped above the occlusion and has no more contact with the ocean.

As the occluded cyclone travels further into the cold polar air masses, cooling of the clouds proceeds, not only moist-adiabatically, but progressively by radiative processes, and we can model the isotopic depletion of the vapour by a Rayleigh condensation. The colder the polar air masses are, as reflected by the surface temperatures, the faster will the isobaric cooling proceed, and in any case, the precipitation will gradually become depleted in heavy isotopes.

The radiative cooling is particularly efficient in winter, when the polar front is displaced southward, and the insolation is minimum. This is an important part of the explanation for the strong annual δ cycle in polar precipitation. Reykjavik is an exception. Throughout the year a substantial part of its precipitation originates from nearby sources with only small seasonal climatic variation, which explains its lack of a seasonal δ cycle (cf. Fig. 4).

Also, the climatic signal observed in δ profiles along ice cores may be ascribed to a southward displacement of the polar front under cold climatic conditions, as it is a common feature of global climatic changes that they are the more pronounced the higher the latitude, and only small in the sub-tropical source area of the moisture (cf. CLIMAP, 1976).

4.5. *The climatic shifts under glacial conditions*

According to Fig. 12, w_{so} in the source area of the moisture determines the slope of the d_p versus $\delta^{18}O$ relationship on the Greenland ice cap, and thereby the slope of the δD versus $d^{18}O$ relationship. Since the latter slope was 8 in both the mild and the cold phases of the glaciation (Table 1), i.e., the same as today (Fig. 7), we conclude that w_{so} in the moisture source region has remained essentially unchanged.

Furthermore, for two geographically different

source regions of the same w_{so}, but of different sea surface temperatures, the model predicts lower d values in ice sheet precipitation from moisture originating in the colder region (Fig. 12). The observation that the deuterium excess was about the same during the cold phases as today, about 8‰, thus indicates that T_s and humidity (R_h) in the moisture source region did not change between the coldest glacial conditions and today. If k in eq. (4) was lower than 6% in glacial times (corresponding to a greater influence of a rougher regime, i.e., stronger winds, as suggested by the high dust contents in the ice cores), T_s must have been even higher in the cold phases than today. In this context, it should be noted that this result for Greenland ice does not agree with the observed change in d found in Antarctica between the last glacial and Holocene. For the Dome C core, Jouzel and co-workers reported a shift in d from 4‰ (last glacial) to 8‰ (Holocene). Their results are, in fact, what one might expect for this climatic transition if the moisture source area(s) did not move in a geographic sense. During the last glacial, ocean surface temperatures were colder in the South Atlantic (CLIMAP, 1976), which explains in part the lower d value in snow. In order to explain all of the observed change in the d value, they further postulated an increase in humidity of 10% at the moisture source area(s). We add here that an increase in humidity of 10%, combined with a cooling of T_s of 2°C, indicates that w_{so} remained relatively constant in the South Atlantic vapour source region(s). In the context of our model, this result implies that the slope of the $\delta D - \delta^{18}O$ line remained constant, a conclusion supported by the Dome C data (J. Jouzel, personal communication).

As to the deuterium excess during the abrupt shifts, the d values of 8‰ in the cold phases and 4‰ in the mild phases of the glaciation suggest that T_s in the source region was at least 2°C *lower* (and humidity about 10% higher) during mild conditions than during cold conditions!

On the face of it, this, as well as the abrupt climatic shifts themselves, might be difficult to comprehend. However, a possible explanation may be sought in the context of the displacements of the North Atlantic Current, e.g., towards south in case of a general cooling, associated with a southward displacement of the atmospheric and oceanic polar front, and of the sea ice border line. In turn, this increased the latitudinal temperature gradients and thereby the zonality of the wind pattern, which had a stabilizing feed-back effect on the North Atlantic Current.

During the cold phases of the glaciation, the sea ice cover advanced to ~45°N in the Atlantic Ocean (Ruddiman and McIntyre, 1981), and the evaporation conditions (w_{so} and T_s) now existing in the Ship E area (35°N), characterized a region some 10° latitude further south, according to CLIMAP (1976). In fact, our findings may be taken as an independent support of the CLIMAP reconstruction of North Atlantic subtropical sea surface temperatures in the late glacial period.

The abrupt shifts to the higher δ's in the mild phases (Fig. 8) might reflect fast retreats of the North Atlantic sea ice cover, which gave a larger contribution of moisture evaporated from open sea water of lower T_s.

The full explanation of such retreats of the sea ice cover implies modelling of the complicated ocean–atmosphere interactions. A hint may be found in the Greenland ice cores, however, in so far as the concentrations of windblown continental dust began to decrease shortly before the cold to mild phase transitions (Dansgaard et al., 1984). This suggests a weakening of the windiness at mid and high latitudes, and thereby decreasing stabilization of the North Atlantic Current, which may ultimately have shifted to a more northerly direction, thereby speeding up the retreat of the sea ice cover.

In the search for an explanatory mechanism behind the abrupt climatic shifts, Broecker (1987) points out that in the present ocean circulation system, cold and salty water sinks in the North Atlantic Ocean, from where it is transported southward by deep ocean currents, via the southern hemisphere oceans, and then northward to the North Pacific Ocean, where some of it upwells. This deep water transport is compensated by surface currents, e.g., the warm North Atlantic Current, a shut-down of which would cool the adjacent lands by 6–8°C. Conversely, re-establishing the present circulation would result in 6–8°C warming. If this were the immediate cause of the abrupt δ shifts under glacial conditions, it might also "explain" the drastic, temporary 10‰ drop in δ at the end of the Eemian interglacial (Dansgaard et al., 1972), see

in Fig. 2 the 10-cm thick ice layer ~29 m above bedrock in the Camp Century core.

5. Conclusion

The deuterium excess $d = \delta D - 8\delta^{18}O$ in precipitation is a parameter that offers additional possibilities for stable isotope studies of processes in the water cycle. We present evidence that, in contrast to low elevation stations, the high elevation areas of the Greenland ice sheet receive precipitation, which mainly originates from subtropical moisture sources, under present as well as under glacial conditions.

6. Acknowledgements

This study was supported by the Danish Commission for Scientific Research in Greenland, the Danish Natural Science Research Council, the Icelandic Sciences Foundation, and the European Economic Communities, XII Directorate General, under contract CLI-067-DK(G). Logistic support for the field work in Greenland was provided by US National Science Foundation, Division of Polar Programs. Support in France was provided by the Centre de la Recherche Scientifique and the Commissariat à l'Energie Atomique.

REFERENCES

Beer, J., Oeschger, H., Andree, M., Bonani, G., Suter, M., Wölfli, W. and Langway, C. C., Jr. 1984. Temporal variations in the ^{10}Be concentration levels found in the Dye 3 ice core, Greenland. *Annals of Glaciology 5*, 16–17.

Broecker, W. S. 1987. Unpleasant surprises in the greenhouse. *Nature 328*, 123–126.

Clausen, H. B., Gundestrup, N., Johnsen, S. J., Bindschadler, R. and Zwally, J. 1988. Glaciological investigations in the Crête-area, Central Greenland. A search for a new deep drilling site. *Annals of Glaciology 10*, 10–15.

CLIMAP 1976. Project members. The surface of the ice-age earth. *Science 191*, 1131–1137.

Craig, H. 1961. Isotopic variations in meteoric waters. *Science 133*, 1702–1703.

Dansgaard, W. 1961. The isotopic composition of natural waters. *Medd. om Grønland 165*, No. 2, 120 pp.

Dansgaard, W. 1964. Stable isotopes in precipitation. *Tellus 16*, 436–468.

Dansgaard, W., Johnsen, S. J., Clausen, H. B. and Langway, C. C., Jr. 1972. Speculations about the next glaciation. *Quat. Res. 2*, 396–398.

Dansgaard, W., Johnsen, S. J., Clausen, H. B. and Gundestrup, N. 1973. Stable isotope glaciology. *Medd. om Grønland 197*, No. 2, 1–53.

Dansgaard, W., Johnsen, S. J., Clausen, H. B. and Langway, C. C., Jr. 1971. Climatic record revealed by the Camp Century ice core. In: *The late cenozoic glacial ages* (ed. K. K. Turekian). Yale University Press, 37–56.

Dansgaard, W., Clausen, H. B., Gundestrup, N., Hammer, C. U., Johnsen, S. J., Kristinsdottir, P. M. and Reeh, N. 1982. A new Greenland deep ice core. *Science 218*, 1273–1277.

Dansgaard, W., Johnsen, S. J., Clausen, H. B., Dahl-Jensen, D., Gundestrup, N., Hammer, C. U. and Oeschger, H. 1984. North Atlantic climatic oscillations revealed by deep Greenland ice cores. In: *Climate processes and climate sensitivity* (eds. J. E. Hansen and T. Takahashi). *Am. Geophys. Union, Geophys. Monograph 29*, Maurice Ewing Vol. 5, 288–298.

Eriksson, E. and Bolin, B. 1964. Oxygen-18, deuterium and tritium in natural waters and their relations to the global circulation of water. *Proceedings of the 2nd Conference on Radioactive Fallout from Nuclear Weapon Tests 675–686. US Atomic Energy Commission. Symposium Series 5.*

Epstein, S. and Langway, C. C. 1959. Oxygen isotope studies. *Trans. Am. Geophys. Union 40*, 81–84.

Finkel, R. C. and Langway, C. C., Jr. 1985. Global and local influences on the chemical composition of snowfall at Dye 3, Greenland: the record between 10 ka B.P. and 40 ka B.P. *Earth and Plan. Sci. Let. 73*, 196–206.

Fisher, D. A. and Alt, B. T. 1985. A global oxygen isotope model semi-empirically zonally averaged. *Annals of Glaciology 7*, 117–124.

Green, J. S. A., Ludlam, F. H. and McIlveen, J. F. R. 1966. Isentropic relative-flow analysis and the parcel theory. *Quart. Journ. Roy. Met. Soc. 92*, 210–219.

Hammer, C. U., Clausen, H. B., Dansgaard, W., Gundestrup, N., Johnsen, S. J. and Reeh, N. 1978. Dating of Greenland ice cores by flow models, isotopes, volcanic debris, and continental dust. *Journal of Glaciology 20*, 3–26.

Hammer, C. U., Clausen, H. B., Dansgaard, W., Neftel, A., Kristinsdottir, P. and Johnson, E. 1985. Continuous impurity analysis along the Dye 3 deep core. *Am. Geophys. Union, Geophys. Monograph 33*, 90–94.

Hammer, C. U., Clausen, H. B. and Tauber, H. 1986. Ice-core dating of the Pleistocene/Holocene Boundary applied to calibration of the ^{14}C time scale. *Radiocarbon 28*, No. 2A, 284–291.

IAEA/WMO, International Atomic Energy Agency/ World Meteorological Organization, 1969–79. *Environmental isotope data No. 1–6*. World survey of isotope concentration in precipitation. *Technical reports series*, Nos. 96, 117, 129, 147, 165 and 192. *I.A.E.A., Vienna.*

Johnsen, S. J. 1977. Stable isotope homogenization of polar firn and ice. Internat. Union of Geodesy and Geophysics, Internat. Ass. Sci. Hydrol., Commission of Snow and Ice. Symp. on Isotopes and impurities in snow and ice, Grenoble Aug./Sept., 1975. *IAHS–AISH publication No. 118*, 210–219.

Jouzel, J. and Merlivat, L. 1984. Deuterium and oxygen 18 in precipitation: modelling of the isotopic effect during snow formation. *Journ. Geophys. Res. 89*, 11749–11757.

Jouzel, J., Merlivat, L. and Lorius, C. 1982. Deuterium excess in an East Antarctic ice core suggests higher relative humidity at the oceanic surface during the last glacial maximum. *Nature 299*, No. 5885, 688–691.

Langway, C. C., Oeschger, H. and Dansgaard, W. 1985. The Greenland Ice Sheet Program in perspective. *AGU Geophysical Monograph 33*, 1–8.

Loewe, F. 1936. The Greenland ice cap as seen by a meteorologist. *Quart. Journ. Roy. Meteorol. Soc. 62*, 359–377.

Lorius, C. 1983. Antarctica: A survey of near-surface mean isotopic values. In: *The climate record of the polar ice sheets* (ed. G. de Q. Robin). Cambridge University Press, 52–56.

Lorius, C., Merlivat, L. and Hagermann, R. 1969. Variation in the mean deuterium content of precipitations in Antarctica. *Journ. Geophys. Res. 74*, 7027–7031.

Lorius, C., Jouzel, J., Ritz, C., Merlivat, L., Barkov, N. I., Korotkevich, Y. S. and Kotlyakov, V. M. 1985. A 150,000-year climatic record from Antarctic ice. *Nature 316*, 591–595.

Majoube, M. 1971. Oxygen 18 and deuterium fractionation between water and water vapour (in French). *Journ. Chim. Phys. 10*, 1423–1436.

Merlivat, L. and Jouzel, J. 1979. Global climatic interpretation of the deuterium–oxygen-18 relationship for precipitation. *Journ. Geophys. Res. 84*, 5029–5033.

Merlivat, L. and Nief, G. 1967. Isotopic fractionation of water during solid-to-vapour and liquid-to-vapour phase shifts at temperatures below 0°C (in French). *Tellus 19*, 122–127.

Ruddiman, W. F. and McIntyre, A. 1981. The North Atlantic ocean during the last deglaciation. *Palaeogeogr., Palaeoclimatol., Palaeocol. 35*, 145–214.

Stauffer, B., Hofer, H., Oeschger, H., Schwander, J. and Siegenthaler, U. 1984. Atmospheric CO_2 concentration during the last glaciation. *Annals of Glaciology 5*, 160–164.

Woillard, G. M. and Mook, W. G. 1981. Carbon-14 dates at Grande Pile: Correlation of land and sea chronologies. *Science 215*, 159–161.

World Survey of Climatology, 1984. Vol. 15. *Climate of the ocean* (ed. H. van Loon). Amsterdam: Elsevier.

Yurtsever, Y. and Gat, J. R. 1981. Atmospheric waters. In: *Stable Isotope Hydrology. Deuterium and oxygen-18 in the Water Cycle* (eds. J. R. Ford and R. Gonfiantini). *Int. Atomic Energi Agency, Vienna, Techn. Rep. Ser.* No. 210, 103–142.